Journal of Intelligent & Fuzzy Systems 44 (2023) 5659–5674
DOI:10.3233/JIFS-221973
IOS Press

An efficient breast cancer detection with secured cloud storage & reliability analysis using FMEA

S. Parvathi[a,*] and P. Vaishnavi[b]
[a]*Department of Computer Applications, University College of Engineering, Anna University, BIT Campus, Chennai, India*
[b]*Department of Computer Applications, Anna University, Chennai, BIT Campus, Tiruchirappalli, Tamil Nadu*

Abstract. Breast cancer is considered as a most dangerous type of cancer found in women among all the cancers. Around 2.3 million women in the world are affected by this cancer and there is no cure if it is left untreated at an earlier stage. Therefore, early diagnosis of this disease is an important consideration to save the life of millions of women. Many machine learning models have been evolved in the recent years for breast cancer detection. However, all the currently available works focused only on improving the prediction accuracy, they need more attention on providing reliable services. This work presents an efficient breast cancer detection mechanism using deep learning strategies. The various assortments like breast image shapes, the intensity of images, regions of an image, illuminations, and contrast are the conceivable factors that define breast cancer identification. This study offers a strong image detection process for breast cancer mammography images by considering the whole slide image. Here, the input process for the preprocessing stage will remove the noise present in the image using Gaussian Filter (GF). The preprocessed image moves to the image segmentation and then forward to the feature extraction for extracting the features of the images using Cauchy distribution-based segmentation and Shearlet based feature extraction. Then the specialized features can be isolated using the Entropy PCA based feature selection. Finally, the breast cancer area is to be detected as benign or malignant accurately by using the Unified probability with LSTM neural network classification (UP-LSTM) for whole slide image (WSI). The attained outcomes and the detected outcomes were stored in cloud using a security mechanism for further monitoring purposes. To provide an efficient security, a Bio-inspired Iterative Honey Bee (BI-IHB) encryption is employed which is decrypted on user request. The reliability of the stored data is then found using FMEA (Failure mode and effective analysis) approach. From the experimental analysis, it is observed that UP-LSTM classifier model offers accuracy of 99.26%, sensitivity of 100%, and precision value of 98.59% which is better than the other state of the art techniques.

Keywords: Breast cancer, Gaussian Filter, Cauchy distribution-based segmentation, Shearlet based feature extraction, Entropy PCA based feature selection, unified probability with LSTM neural network classification, FMEA (failure mode and effective analysis), benign, malignant, histopathology images, WSI, cloud security, bio-inspired iterative honey bee (BI-IHB).

1. Introduction

Around the world, Breast cancer is regarded as one of the important cancer-related death causes in women. In accordance with Canadian Cancer Society, about 26,000 women were spotted with the breast cancer in Canada in the year of 2017 which signifies all new cancer cases in women [1] around 25%. In the same year in Canada, about 5,000 women lost their lives because of breast cancer in women that denotes about 13% of all types of cancer deaths. Early diagnosis can be helpful in treating the disease without loss of life [2]. The signs and symptoms of breast cancer were varied and the diagnosis will

*Corresponding author. S. Parvathi, Department of Computer Applications, University College of Engineering, Anna University, BIT Campus, Chennai, India. E-mail: 5680sparvathi@gmail.com.

ISSN 1064-1246/$35.00

comprise biopsy, mammography, physical exam, and ultrasound testing. Biopsy is usually done once after the diagnosis of some irregularity with the use of ultrasound and mammography [3]. In biopsy, a tissue sample is removed surgically to be examined. This can point out which type of cells is cancerous, and also the cancer type these were related to. Microscopy imaging biopsy sample data are complex in nature and large in size. Consequently, pathologists will face an increase in workload substantially for the diagnosis of histopathological cancer. In recent days, [4] the growth of computer aid diagnosis (CAD) systems helps in the reduction of workload. Digital pathology continues to increase energy wide-reaching for diagnostic purposes. Nowadays, techniques of deep learning were developed for solving quite a lot of problems in the area of medical image processing [5] CNN is regarded as the better solution for solving classification problems once the input is high-dimensional data like images.

Diagnosis and outcome prediction are two areas that may benefit from the application of ML techniques in the medical field. It involves the likelihood of recognizing elevated risk for patient conditions, such as deterioration in health or transition to another disease [6]. The different learning paradigms with machine learning are unsupervised, reinforcement, and supervised learning [7]. In supervised learning, the model learns through the labeled dataset and predicts the nature of the unknown output. Classification and regression problems come under supervised learning. Classification problems deal with predicting discrete values whereas continuous data is predicted by regression problems. In unsupervised learning, the model is not given labeled dataset instead it investigates the underlying pattern and predicts the output. In reinforcement learning, an agent, for its every attempt, is rewarded for success and penalty for failure. Thus, the agent learns from the environment. The unique characteristic of the machine learning model is that if the prediction goes wrong, the data analyst can step in and make corrections. On the contrary, another model called deep learning model, a subset of machine learning model, wherein an algorithm will decide on its own whether or not the prediction is correct with its own neural network. In this work, both machine learning and deep learning models are applied to diagnose the type of breast cancer.

The most commonly reported cancer in women kind is breast cancer, according to the world health organization [8]. Almost 2.1 million women are subjected to breast cancer and on an average about 627,000 women died every year. The two types of breast cancer are malignant and benign. The most remarkable benign and malignant tumor characteristics are listed in Table 1.

Table 1 clearly reveals that if breast cancer is identified at a benign stage, the possibility to improve the life span of the patient increases whereas if developed into malignant, the cells multiply and grow in the breast tissue beyond the control making the patient life miserable [9]. There are many risk factors for developing breast cancer in women. Some risk factors such as aging, life style, and family history are beyond the control that no one cannot change. On the other hand, some are related to the lifestyle such as alcohol consumption, obesity after menopause, lack of physical activity, having no child or having a first child after age 30, not breastfeeding, etc. [10]. Breast cancers can also be found in male but the probability of occurrence is too low.

In 2020, according to American Cancer Society, the estimated number of breast cancer cases in US is 279,100, out of which, 42,690 are estimated deaths [11]. The incidence rate of breast cancer is increased by 0.3% every year from 2007. The death rate is 33.2 per 100,000 in 1989 and reduced dramatically by 40% in 2017 [12]. This achievement is due to the increased awareness as well as early detection of disease. The most reliable method to detect early stage of breast cancer is undergoing regular breast cancer screening. Women who crossed the age of 40 must have mammogram screening every year. To address the false positive rate in breast cancer screening with mammograms, biopsy imaging is done finally to confirm the presence of cancer [13]. When the mammogram or other imaging techniques such as Ultrasound, MRI suspects the presence of cancer, breast biopsy is done finally, which is the one and only way, as of now, to confirm the presence of breast cancer. During biopsy, the small amount of tissue is taken from the suspected area and undergoes laboratory test to confirm the presence of cancer cells. Depending upon the size, location, and number of cancers present, the type of biopsy can be selected. From each cell in the sample, ten features such as radius, texture, perimeter, area, smoothness, compactness, concavity, concave points, symmetry, and fractal dimension are computed. For all such features, its mean, standard error and the largest or worst values are computed rendering 30 features along with patient ID number and diagnosis. The dataset, downloaded from UCI machine learning repository, is used as a benchmark database for breast cancer prediction [14]. Many research works are car-

Table 1
Benign and malignant tumors characteristics

	Benign tumors	Malignant tumors
Cells	Similar to normal cells	Varied in size and shape with large nuclei
Growth	Relatively slow and frequently encapsulated	Rapid growth and no capsule
Spread	Remains localized	Invades nearby tissues
Life threatening	Not in all locations. But its location in mammogram is risky.	Yes, by tissue destruction and spread of tumors

ried out to identify the early stage of cancer and to save human life. Advances in cancer detection and treatment increase the longevity of the patients. Data visualization is an excellent way for users to quickly read and interpret data, particularly in broad data analysis [15]. Visualization often helps researchers to understand trends and associations across vast quantities of data that cannot be readily expressed across raw data. In this work, we considered the WSI using mammography images to carry out the breast cancer detection process. Entropy PCA based feature selection is used for efficient feature selection. Then, UP-LSTM model is used for the classification of breast cancer. The unique part of the work is the preservation of results using cloud based strong security mechanism. To achieve this, the results are stored in a cloud with the help of Bio-inspired Iterative Honey Bee (BI-IHB) encryption mechanism. The performance of the breast cancer identification experiments are carried out using MATLAB by taking BreakHis breast cancer dataset and the outcome of the experiments proved the efficiency of the proposed work compared with the other conventional breast cancer identification techniques.

The remaining sections of the article are organized as follows. A literature review containing recent related studies on the detection of breast cancer is provided in Section 2. The methods and the application of the proposed method to the dataset are elaborated in Sections 3 and 4. The last section exemplifies the results, comparative analysis and discussion.

2. Related works

Globally, the breast cancer incidence rate has been increasing significantly day by day. To save the lives of women across the globe, many researchers are struggling to address the early detection of breast cancer using recent advanced techniques. Machine learning is one such technique applied for breast cancer detection. Breast cancer Wisconsin dataset is used as a benchmark database for the research community. This section deals with a detailed survey of various machine learning techniques applied on Wisconsin breast cancer diagnostic dataset.

Authors of [16] proposed simultaneous feature selection and classification using genetic programming and achieved 98.24% with 6.52 average features. In [17], the work investigated the efficiency of six machine learning algorithms such as C4.5, Random Forest, KNN, Neural networks and SVM. In their research, the introduction of k-means algorithm to identify the concealed patterns of benign and malignant tumor as a first step followed by building SVM classifier improved accuracy to 97.38%. Also, various machine learning and deep learning models and concluded deep learning models outperformed machine learning models were implemented by giving an accuracy of 99.3%. Authors of [18] did a comparative study using ANN, KNN and Naïve Bayes classification algorithms and proved that ANN is performs well for cancer detection with the obtained results of 97.4% accuracy in 3-fold cross validation. In [19], the comparison of neural network and deep neural network with and without dimensionality reduction techniques such as Linear Discriminant Analysis (LDA) and Principal Component Analysis (PCA) is performed. They got maximum accuracy of 97.06% from the Neural network with LDA.

In [20], the authors of the work compared the performance of four algorithms such as decision tree J48, REP Tree, Random forest and Priority based decision tree algorithm. The simulated results proved that priority-based decision tree classifier performed well with 93.63% accuracy.

In [21], the work suggested a new deep cascaded CNN convolution neural network that comprises of two techniques. initially, the CNN leveraging which is the coarse model for the recognition of mitosis candidate and their localization for the conservation of sensitivity rate.

Authors in [22], presented a narrative histopathological image breast cancer technique intended for categorization based on the deep CNN that is termed

as model BiCNN, meant for the breast cancer classification addressing with two-class on the pathological image. This representation depends on deep learning that has both labels of breast cancer of class and subclass since a prior information which in turn controls the distance feature descriptions of the breast cancer pathological image.

In [23], the authors stated an approach of deep learning for the visual analysis and automatic detection of tissue regions invasive ductal carcinoma (IDC) in WSI of the breast cancer (BCa). Deep learning approaches are methods of learn-from-data that involves modeling of the computational learning process. This technique was related to the way of human mammograms work with the use of diverse understanding layers or levels of most useful and representative features resulting from the representation of learned hierarchical depiction.

Authors of [24] considered a unified structure for the prediction of tumor propagation score from the breast histopathology entire slide images. This system in turn recommends a completely automatic result for the prediction of both data-based molecular, and a counting-based mitosis proliferation score of tumor. The structure integrates three modules, all fine-tuned to exploit the whole performance: An image processing part for managing entire images of slide, a deep learning dependent detection of mitosis, and a propagation scores prediction component.

Authors of [25], proposed the classification of malignant and non-malignant cell structure coefficients using Support Vector Machine (SVM). The *support vectors* have been determined by the *Lagrangian multiplier* with *labelled+1* and *–1* variables using binary classifiers, but the problem is that the cell structure extraction has not been described very well. Therefore, the work found the direction of gravity *gradient vector* using differential operation. It has been very much useful to identify the centre of the cancer cell and its direction variations using *principal components* (PC). These methods have failed to detect the direction of cancer cell, due to the variation of irregular-shaped malignant and various types of cancer cell patterns in the image. In Neural Network (NN) perspective, the work] have combined the *AdaBoost classifier* and WT technique to identify the cancer cell structure, particularly in the spindle nucleus cell detection. The non-malignant based feature components have been detected using *AdaBoost classifier* and the nucleus cell detection-based feature coefficients are detected using WT technique. These methods often identify the cancer cells in breast tissue images and the irregular cell structure is detected using stability and symmetry of the malignant region.

[26] proposed the initialization of potential biomarkers to enable reliable and reproducible biomarkers across the several expressions of genes. They describe the gene expression through the Data-Driven Reference (DDR) approach to eliminate the platform-based biases and the non-biological variable factors.

[27] presented a novel (CNN) based prearranged regression model that is exposed to be competent of handling moving cells, inhomogeneous environment noises, and huge variation in shapes and sizes. The projected technique only needs a few training images by means of weak observations.

[33] proposed a MRR prediction using deep learning strategies for product quality control with the help of residual CNN and the experimental analysis proves the efficiency of ResCNN for the prediction of MRR.

[34] proposed a prediction of RUL with the novel idea of self-learned weights. The outcome of the work shows the superiority than the other deep learning approaches.

3. Proposed work

The proposed mechanism and its overall workflow are described briefly in this section. In this work, the breast image dataset image preprocessing, segmentation, feature extraction, feature selection, and classification are processed. Initially, the image is preprocessed and Gaussian filtering is applied to enhance the quality of image. The flow of the proposed system is shown in Fig. 1. The Cauchy distribution-based segmentation process is employed for image segmentation. The features are then extracted using Shearlet based feature extraction and the optimal features were selected using Entropy based PCA. The unified probability with LSTM neural network is applied for the purpose of classification. Thus, the classified breast mammogram image is attained and the classification of cancerous and non-cancerous regions was predicted.

Finally, the classification of image was done and the results are evaluated by comparing it with other existing methodologies.

3.1. Preprocessing based on Gaussian filtering

The proposed disease prediction model is shown in Fig. 2. Initially, the dataset was pre-processed

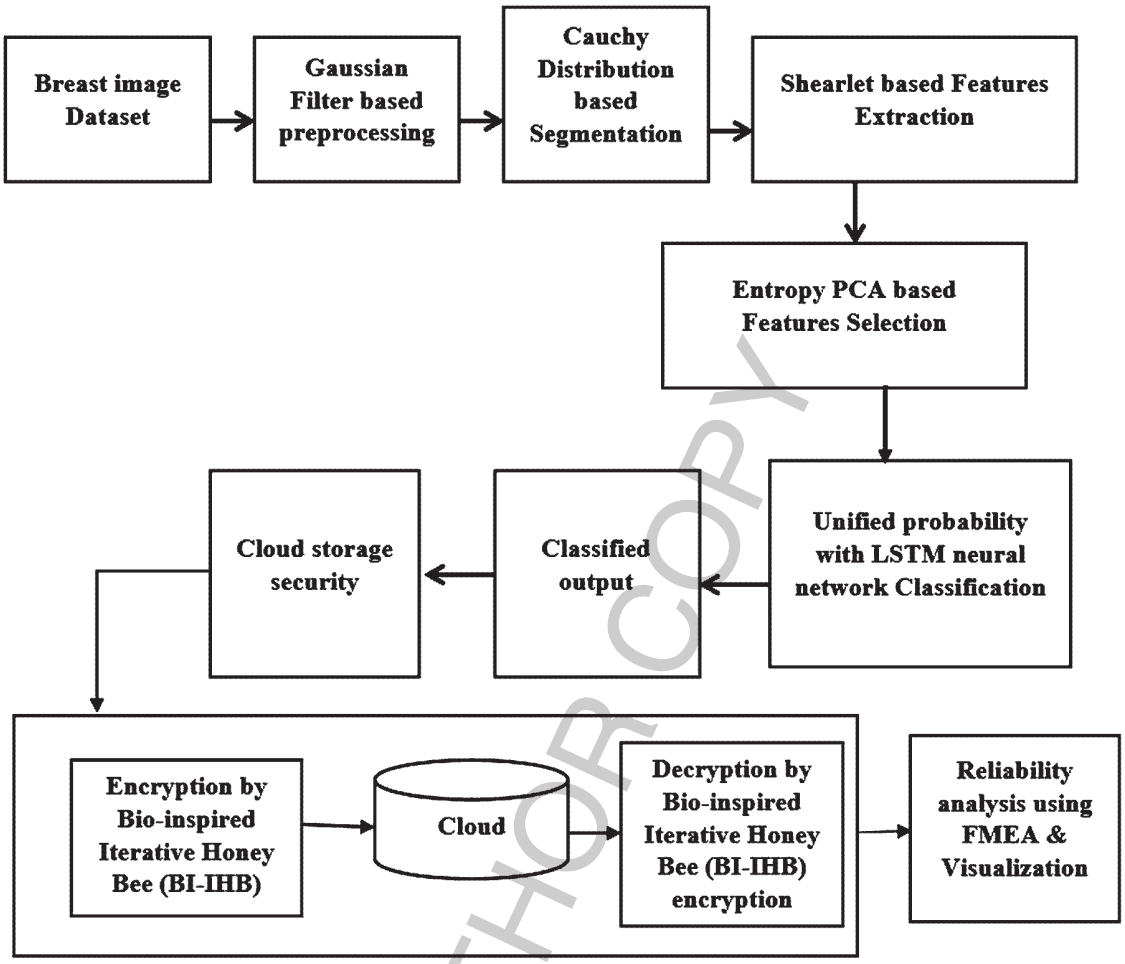

Fig. 1. Flow of the proposed strategy.

in order to remove excess noise in the image. The noise presence will affect the overall image quality. Thus, to enhance the quality of the image and to get a better result on further processing of an image, pre-processing is done. There are different types of noise exist in medical image and Gaussian filter is a good choice for image processing while considering internal and external factors of the image. Speckle Noise may exist in the digital images and MRI images because of some external and internal factors. Gaussian filter can be utilized to remove the Speckle Noise in the images such as ultra sound images or MRI images. Here, the noisy pixel in the image is replaced by average value of the surrounding pixel or neighboring pixels which is based on Gaussian distribution One benefit of using Gaussian filter is that it is faster than other techniques such as median technique because multiplying and adding is probably faster than sorting. The next step involves the scanned images preprocessing with the use of filtering method. In this approach, Gaussian filter is used mainly to smooth the textures, conserve the boundaries, and in reduction of Gaussian noise. The average of weighted intensity from the neighboring pixel was positioned in every pixel of the image. The weight is based on pixels Euclidean distance and also on the radiometric dissimilarity that is depth distance and color intensity.

The filter relation can be given as

$$BF[I]_p = \frac{1}{w_p} \sum_{p,q \in s} G_{\sigma s}(||p-q||) G_{\sigma r}(||I_p - I_q||) \quad (1)$$

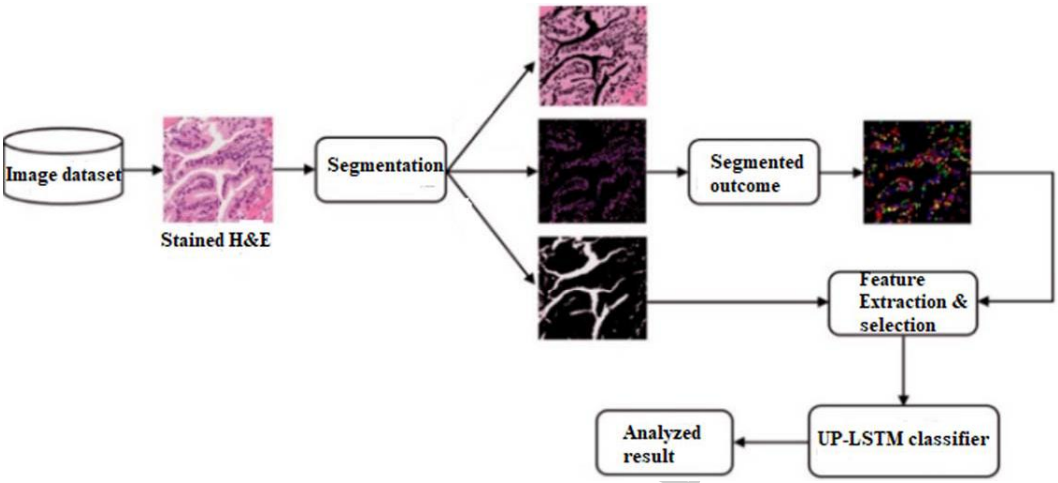

Fig. 2. Graphical representation of proposed disease prediction flow.

$$G_\sigma(x) = \frac{1}{\sigma\sqrt{2\pi}}\exp\left(\frac{-x^2}{2\sigma 2}\right) \quad (2)$$

Where Wp is normalization factor, G$\sigma s$is normalized weighted average, I represent image, $\sigma sand\sigma v$ are the filtering parameters.

Such noise reduction is a typical pre-processing step for better performance. In general, the X-ray image comprises of three (red, green, blue) channels. The blue channel loses its greatest clarity and contrasts sharply. Second, during preprocessing it blocks the green channel. Typically, poor contrast occurs with x-ray objects. Preprocessing is performed to increase the green channel's contrast. Typically, histogram equalization is done to improve the image quality. Histogram Equalization is a computerized technique used to increase the contrast of images. It is achieved by effectively growing the most normal intensity values, i.e. by expanding the picture intensity range. there was an indifference. The distinction between areas is rendered fewer local in contrast. Thus, the average image contrasts are increased by following the histogram equalization, which is a process that requires intensity adjustment, thus increasing contrast, indicated by P as the uniform histogram of an image for each possible intensity.

$$\text{Histogram equalization (P)} = \frac{\text{Intensity sum of the pixel}}{\text{Pixel average number}} \quad (3)$$

This method can be used for improving image quality with histogram equalization. Then, by changing the RGB values, the sensitivity may then be calibrated.

3.2. Cauchy distribution-based segmentation

Segmentation is the process of partitioning a digital image into multiple segments (sets of pixels, also known as image objects). Image segmentation is typically used to locate objects and boundaries (lines, curves, etc.). This subsection is envisioned to deliver a transitory overview on the Cauchy distribution approach. The Cauchy distribution is regarded as a special circumstance of SαS family. Unlike SαS distributions which lack in a condensed logical PDF expression, the univariate Cauchy distribution has the PDF defined as

$$p_\gamma(x) = \frac{1}{\pi}\left[\frac{\gamma}{(x-\delta)^2+\gamma^2}\right] \quad (4)$$

where δ is regarded as a location parameter, which in turn specifies the peak distribution location and γ is the distribution dispersion that regulates the distribution spread over their parameter location. In the stage of region merging, estimate the features of the region were estimated using a symmetric function of the Cauchy density having zero mean (δ=0). The detail coefficients histogram in a specific sub band is formfitting by the Cauchy model assessed in evaluation with the fitted generalized Gaussian distribution (GGD). By means of investigating the graphs, the coefficient distribution of the sub band slowly decays on tails together. The model of Cauchy delivers an improved fitting on these substantial tails on comparing the comprehensive Gaussian archetypal. This has been substantiated by the KLD to estimate the transformation among two probabil-

ity distributions. The smaller value designates an improved fit.

The isotropic bivariate Cauchy distribution is an associate of the multidimensional isotropic stable distribution's family, whose PDF could be inscribed as

$$p_\gamma(x_1, x_2) = \left[\frac{\gamma}{2\pi\left(x_1^2 + x_2^2 + \gamma^2\right)^{3/2}}\right] \quad (5)$$

where the parameters of location are expected to be zero by means of the supplementary progress in the wavelet analysis framework. This model is employed in segmentation stages which in turn offer higher outcomes by means of not only taking the behavior of the heavy-tailed sub band peripheral distribution, but likewise the robust statistical dependences among wavelet coefficients at dissimilar scales. After segmentation, features are extracted from the segmented images.

3.3. Shearlet based feature extraction

Then the features can be chosen by using the Shearlet approach following the segmentation step. This is a means of removing second-order mathematical texture characteristics. This technique has been utilized in several applications, whereas the interaction of three or more pixels occurs with higher-order textures. This is a mathematical task that will typically eliminate the objects efficiently. The accuracy of the image may also be rendered clear. The image may be differentiated during the analysis cycle. In a particular exact differential area, Shearlet can specify the frequency of the pixels. The single-pixel is to be questioned here, and another pixel is known as the Ø route l and the adjacent value detachment of m. Usually, m obtains a single value, and Ø can benefit directionally. Then the obtained directional value can remove the attributes of the images used for the segmentation process. The Shearlet process may be set as follows:

$$K(m,n) = G(m,n,o,Ø)/\sum_{m=1}^{H}\sum_{n=1}^{H} G(m,n,o,Ø) \quad (6)$$

Where G is the frequency vector, m, n, ois the frequency of the particular component will generally having the pixel values of l and m, K represents the features of an image, (m,n) was the component of the m and l, Ø represents the normalized constant.The various attributes can be obtained by applying the Shearlet approach. Then the features can be viewed by the PCA method.

3.4. Entropy PCA based feature selection

Steps for feature selection is shown in algorithm 1. An entropy-based feature concerned for different purposes narrated to the biomedical field-based image processing. Entropy is the measurement of randomness degree that can be used to characterize the texture of an input image. By computing the entropy or uncertainty of the preprocessed image, the information content of an image is frequently computed. Moreover, more information is associated with the preprocessed image, as the amount of entropy gets increases. In addition, the entropy performs average estimation to the information of global image content about average bits per pixel. The distribution probability enabled measurement of entropy defined as given below:

$$E = \sum_{J=0}^{N} x_j log_2 x_j \quad (7)$$

This equation is the Shannon entropy and
Where, x_j is jth pattern probability

Algorithm 1: Feature selection

Input: input images for the extraction of features τ_{fs}
Output: Selected features φ_{cnn}
Step 1: $\{\tau\}_{fs} \leftarrow\leftarrow$ the population is initialized with projected gene encoding approach;
Step 2: t $\leftarrow$ 0;
Step 3: **while** criterion of termination is not contented do
Step 4: Estimate the individual fitness of τ_{fs};
Step 5: S $\leftarrow$ Choose parent solutions along with selection of slack binary tournament value k (which determines the optimal solution for each parent)
Step 6: $\varphi_{cnn} \leftarrow$ Generate off springs with the designed genetic operators from S;
Step 7: Pt + 1 $\leftarrow$ selection of parameter from $\varphi_{cl} \cup \varphi_{cnn}$t;
Step 8: t $\leftarrow$ t + 1;
Step 9: **End while**
Step 10: Select the preeminent individual from φ_{cl} and decode it to the consequent neural network.
Step 11; **End**

It is praiseworthiness to observe that the entropic logarithmic assessed as x_j tend to 0 their self-analogous information to their events, $I(x_j)$=-log (x_j) tend to perpetuity($x_j = 1$)=log x_j tend to 0. Therefore, it is seen that the gain of information for an occasion is neither bounded at together sides nor distinct at the entire points. Actually, for an event the information gain, also extremely uncertain or probable, is predictable to lie down among two definite limits that is, as the maximum number of image pixels

were analyzed, the increase in gain of information so that the entire pixels were analyzed as the gain attain their utmost value, irrespective of image essence. The entropy-based feature selection done by establishes the preprocessed breast image data and also for uniformity of histogram helps to calculate the feature selection as given below:

$$\mathrm{E} = \sum_{i=0}^{u-1} p\,(i)\, log_2[\mathrm{p(i)}] \tag{8}$$

For example, if the entropy gets calculated for 2 variables, the equation gets written as,

$$\mathrm{E} = \sum_{a=0}^{u-1} \sum_{b=0}^{v-1} p\,(a,b)\,.log_2\,[P\,(a,b)] \tag{9}$$

For the image recognition, the feature selection algorithm depends up on the entropy, which is appropriate in larger Signal-to-Noise Ratio framework. Though, when the signal is entirely immersed in the noise, the recognition process depends on the signals difficulty by entropy uniqueness is difficult when the identifying the signals as accurate manner by reason of the large overlap time among the several signal entropy uniqueness. By concerning the above entropy-based feature selection, the amount of entropy values increases and the extraction of features get selected for further image classification.

This is one of the most commonly employed methods in extraction. It shows the highest volatility in extracting the most relevant features from the data. This PCA-based selection method determines whether the quality of the breast images is beneficial or not. The criterion value of the form used by certain correlation parameters is based on the absolute and partial association of the breast images. The key usage of PCA in histopathology breast image is to evaluate the functionality of the input of regulated and unregulated classification applications. The overall method depends on device load and the change in input and failure detection performance. The revised artifacts in the collection cycle are produced by using the feature extraction procedure. Instead of their conceptual quantity as seems to be mostly sufficient for binary image processing, rational operations depend more on numerical sorting of images. Morphological behaviors may also be broadened to involve grayscale pictures, meaning that they do not recognize their light propagation mechanisms and thus have little to no experience in their individual pixel values.

After the segmentation of region, the feature extraction and selection of best features are carried out with the use of PCA approach. so as to guarantee the features a useful one of the classification purpose, PCA is introduced for the extraction of global grayscale feature and thereby reducing the size of data. From this, the optimal features are selected with the use of feature selection process.

The selection process makes the classification approach a simple one and also it is helpful in the better enhancement of classifier outcomes. Tournament selection determines the best solution among all the possible solution.

3.5. Unified probability with LSTM neural network classification

A Unified probability with LSTM neural network has the input parameters of single input layer, a hidden layer, and an output layer. The basic unit of the secret layer is memory cube, unlike the conventional neural network. The memory block contains memory cells that save time which have a pair of adaptive multiple gating devices in the block in order to monitor the flow of information. The activation input and output of the block is regulated in two ways by the source of input and output. The memory cell activation can be done initially. Due to this the suggested correlation feature based LSTM can solve the fading error issue by maintaining the error constant. Steps for Unified probability with LSTM is shown in algorithm 2. After the activation of the memory block the selected features can be given as an input for the process. The memory blocks are allowed to reset by themselves as the flow of information becomes redundant and the error input weight is replaced by the weight source activation. The training sequence in which forward and backward to two distinct repeating networks, which is both related to the same performance stage, is the basic principle of the proposed classifier. This implies that the grouping of all points before and after each point of a specific series has maximum sequential knowledge.

step 1: Use N of random training set data points.

step 2: Decision tree can be built depending upon the N points

step 3: Choose the exact replicate from phase 1 and 2 from that can be used to build a decision tree.

step 4: Create a unified probability based trusted value

The Unified probability with LSTM neural network generates a collection of breast dataset. This

Algorithm 2 (Unified probability with LSTM neural network classification)

Input: Specialized features S_f
Output: Classified data C_{datas}
Initialize the multi-Network layers
Initialize train features
Initialize label
Train label = 80%
Test label = 20%
Label = unique(label)
For i = 1:lengh(label)
Class = find (label==test (i))
Traincut = length(class)-traincut
Traindata = [traindata; trainfeatures;class(1:Traincut)
end-5:end]
Predict label = classify(net,traindata)
End For
For j = 1:size(traindata,1)
Train data = [train data; train features; class(1:Traincut)
end-5:end]
End For
For k = 1:size(trainfeatures,1)
Train data = [train features; train features; class(1:Traincut)
end-5:end]
End For

combines votes of classifier subsections into a single word and then settles on the final test entity category. For calculating the trusted classified value, the Unified probability with LSTM neural network for predicting the harmful disease in the histopathology image has to be calculated. Here in which the Unified probability with LSTM neural network parameters can be calculated,

$$C_f(\mathrm{i}) = \begin{cases} c_{f_{min}} + \left(c_{f_{max}} - c_{f_{min}}\right) * n, n < 1 \\ c_{f_{max}/} N_{iter}, \end{cases} \quad \mathrm{i} = 1 \ldots \mathrm{n} \qquad (10)$$

where f = fitness(i) - f_{min}, which depends on the current quality of ith solution

After that the parameter gets initialized and the abnormality gets analyzed.

$$\sigma_v = (\gamma\,(1+\beta_c))^{*}\sin(\pi *)/(\gamma\,(1+\beta_c 2)^{*}\beta_c^{\beta_c - 1/2})*$$
$$= (\gamma\,(1+\beta_c))^{*}\sin(\pi^{*})/(\gamma\,(1+\beta_c 2)^{*})^{*}(\beta_c - 1/2)^{1/(\beta_p - 1/2)} \qquad (11)$$

Where σ_v represents the random size of the nest.

$$\text{Correlation (i,j)} = \sqrt{(C_{n_{fea}}(i,1) - V_{n_{fea}}(j-1)) + (C_{n_{fea}}(i,1) - (C_{n_{fea}}(j,1)^2} \qquad (12)$$

As the prototypes are conditioned on normal and abnormal values depend upon its abnormal features. Here the probability can be calculated by using the equation (14)

$$C_{n\_prob} = [C_{n\_prob}\mathrm{unif}] \qquad (13)$$

Hence the classifier can evaluate the probability of abnormality and can discriminate the breast cancer and its grading according to the grade level. Then the trust value can be calculated for the classification of the breast image.

$$C_{tv} = (C_{n\_prob} dist) \qquad (14)$$

Where C_{tv} represents the trusted value of the beast image data. Depends upon the trusted value the breast abnormality can be identified.

By concerning these processes, to attain the score value, which is effectively choose either the particular image is breast cancer or not. If the score value surpasses the threshold value, it denotes that the precise interference i.e., normal image.

Decision = $T_h \geq$ score value, cancerous region

$T_h <$ score value, non-cancerous region

If the threshold value is lesser than or equal, the particular image considered as the cancerous region. The computed score value assessment by concerning the above given condition.

3.6. Cloud Storage using Bio-inspired Iterative Honey Bee (BI-IHB) encryption and decryption process

Encryption

The predicted resulted images are stored in a cloud environment which is received from classification. So, keeping these results is the important priority in cloud. To enhance the data security, cryptography-based algorithm is proposed. This process is done primarily by admin. This is one of the most widely used cryptographic algorithms which extend security, based on the complexity of varied problems involved. At the beginning, user encrypts the data before transmitting through cloud. For the purpose of encrypting data, the enhanced honey bee algorithm is proposed. Once encryption is done, the content presented in data cannot be viewed without decrypting it. The data size is the most important for encryption. Keystore was kept in cloud as normal for further encryption. Steps for encryption process is shown in algorithm 3.

In this proposed algorithm, the classified data are encoded and stored in "s". It receives these data as "0"s and "1"s. Here, plain text is assigned as a Cipher text. Then, it returns to "r" variable.

Decryption

The encrypted information can be accessed by authorized persons only. This information is required to decrypt for authorization. Just like encryption the decryption is carried out based on honey bee decryption. Decryption is the process which modifies the encrypted information into a meaningful frame. To switch from encryption, decryption key / decoding key is used. If the decrypted key is lost, then the data will not be decoded. So, it should be protected legitimately. Bio-inspired Iterative Honey Bee (BI-IHB) algorithm has been employed in implementing decryption. In this enhanced algorithm, the stored information is decoded as a message. The information security is required to secure the information from the third part view and other unauthorized hacks. Thus, the information stored in the cloud can be extracted for further monitoring and diagnosing purpose.

The data stored in the cloud is then tested for reliability at which there is a risk on fault identification. thus, the predicted output is being checked for reliability to ensure sensitivity rate of the detected output using Failure mode and Effective analysis (FMEA) system.

Cloud storage is important to store all the disease related data for further processing. It also supports cost effective solution and are more efficient. Because of the integration of cloud, the cloud server can perform the prediction process efficiently and cost can be reduced ensuring the enhanced detection.

3.7. Failure mode and effective analysis (FMEA) for reliability analysis

Failure Mode and Effective Analysis (FMEA) is used to eliminate or reduce the failures based on system highest priority. It is a structured and bottom-up approach to effectively reduce the potential failures. Each system contains several functional components for different purposes and each are designed for specific applications. FMEA is detecting the potential failure of detection system and most of them are due to failure in intended process. It used to identify the Severity ratings (SR), failure Occurrence (O) and number of times it can be Detected (D). Severity ratings (SR) are considered for worst case machine failure, property damage or system damage. These failure details are recorded and stored as a historical fault record that helpful for analyzing future failure. Similarly, the Occurrence (O) of failure is also measured and used to estimate the potential ability of problem occurrence. Finally, based on the number of occurrence the failure Detection (D) is confirmed. FMEA is involves evaluating current maintenance program in order to eliminate the redundant actions and ensures the effective maintenance. This process is calculating Risk Aid Number (RAN) for failure mode. The RAN is measured as a product of these three failure factors such as Severity (S), Occurrence (O) and Detection (D) and assumes these three has equal priority in calculation. Consider the number of failure is defined as i and failure mode number as $i = 1, 2, 3,.N$. For higher value of RAN (Risk Aid Number), the system has greater risk of failure whereas lower RAN value the system has lower risk of failure. With the help of assigning Risk Aid Number (RAN) which results in control and maintenance of production management. Risk Aid Number (RAN) can be calculated as

$$RAN = \sum_{i=1}^{N} SriXOiXDi \tag{15}$$

Where $i = 1, 2, 3 \ldots$ N.

After identification of risk analysis in the detection system and reason for that failure by FMEA process next performance evaluation phase will be started. thus, the reliability of the system is found using this FMEA approach.

4. Performance analysis

The performance estimation of the proposed mechanism is shown in this section. also, the comparative analysis of the proposed system along with existing techniques were evaluated and the outcomes were shown below.

4.1. Dataset description

In this approach, the work uses BreakHis [27] breast cancer dataset for the evaluation of proposed system robustness. The dataset BreakHis comprises of 7909 benign images and the histopathological malignant images are 1,370 and they are gathered from 82 patients. The histopathology images were attained with the use of dissimilar factors of magnification in this dataset like 40x, 100x, 200x, and 400x. The presented models have employed the entire histopathology images available devoid of taking magnification factors into consideration for classifying the histopathology images as malignant and benign category. The malignant and benign sample

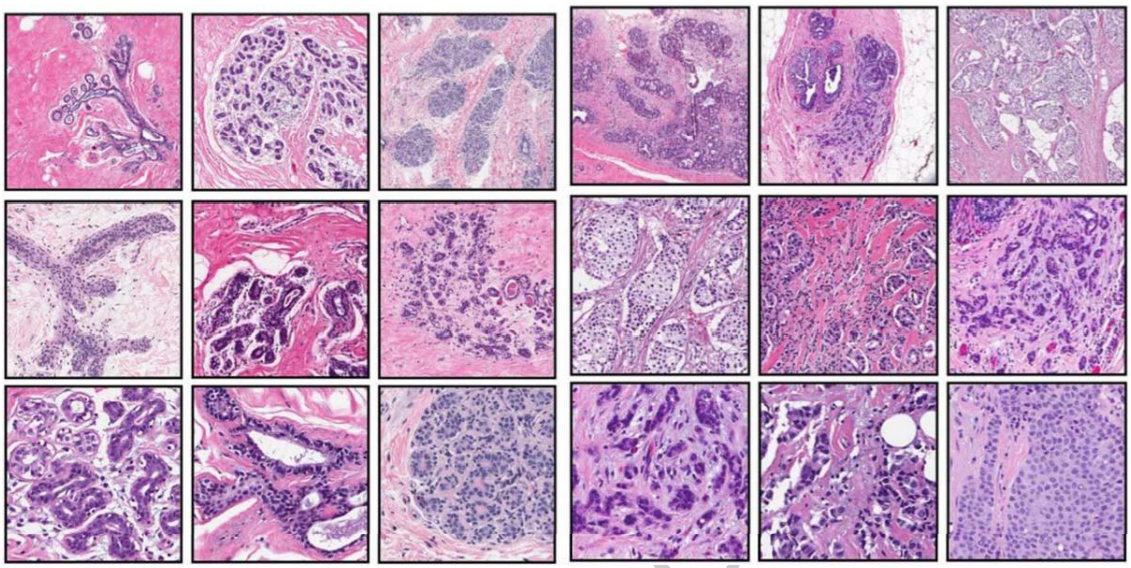

(a) Benign (b) Malignant

Fig. 3. Sample images of benign and malignant classes of BreakHis database.

classes images are exposed in Fig. 3. Patient level and Image-level criteria of image were employed for the sample database. At the Image-level technique, 80% of magnification independent histopathology images were employed for training and 20% of them were employed as test data.

4.2. Experimental analysis

The work uses BreakHis dataset which is separated for testing and training sample pool. While perform testing, the work guarantee that it has balanced benign and malignant samples. The imbalanced samples are resolved through rotational augmentation on the samples. The images are resized to 227 x 227 before giving as the input to the network. Then we use AdamOptimizer to update the parameters. Once the training process is over, the parameters are fine-tuned when the data is high to perform classification. The confusion matrix is shown in Fig. 4 calculates the parameters such as true positive, true negative, false positive, and false negative. Correctly predicted as positive instances are called true positive (TP), correctly predicted as negative instances are called true negative (TN), number of predicted positive instances as negative are referred as false positive (FP), and the number of predicted negative instances as positive are referred as true negative (TN). The common performance metrics used in this calculation are sensitivity, specificity, F-score, precision, and accuracy.

Accuracy

This defines the ordered errors, and calculate the composition's arithmetical field. Low accuracy creates a disparity between a measurement and a "real" value. This ensures that the exceptional data samples are checked using the same algorithm many times and the computer or device produces correct tests. The exactness of the final details is the percentage of the real results.

$$\text{Accuracy (A)} = (\text{TP} + \text{TN}) / (\text{TP} + \text{TN} + \text{FP} + \text{FN}) \quad (16)$$

Sensitivity

Sensitivity is often referred to as the actual positive degree identification. The percentage of real positives accurately detected is calculated by certain sectors.

$$\text{Sensitivity} = \frac{\text{TP}}{(\text{TP} + \text{FN})} \quad (17)$$

Specificity

Specificity, also known as the real negative score, calculates the amount of individual negatives accurately defined.

$$\text{Specificity} = \text{TP} / (\text{TP} + \text{FP}) \quad (18)$$

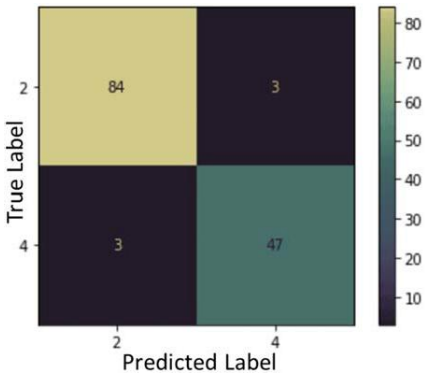

Fig. 4. Confusion matrix.

Precision

Precision is a portrayal of random errors that is a measure of algebraic variability.

$$\text{Precision} = \text{TP}/(\text{TP} + \text{FP}) \quad (19)$$

F-measure

The harmonic mean of precision and recall was the F-measure.

$$\text{F} = 2*[\text{Precision}*\text{Recall}]/\text{Precision} + \text{recall} \quad (20)$$

Balanced Accuracy (BAC)

Balanced accuracy is estimated as the proportion corrects of each class individually average. In this instance, both the balanced and overall estimations yield the same accurateness, as will happen always once the test set consumes the same number of instances in each class.

$$\text{BAC} = ((\text{SEN} + \text{SPE})/2) \times 100 \quad (21)$$

4.3. Empirical analysis of proposed and existing techniques

This section is the depiction of comparative analyses of the proposed and existing techniques performance to prove the robustness of proposed system as shown in Table 2.

Figure 5 is the graphical representation of the classifier performance and Fig. 6 is the representation of prediction maps for WSI samples in the test set that were obtained using UP-LSTM classifier system. The original WSI image, their annotated patches, and the prediction maps were shown.

The performance estimation is made and the proposed UP-LSTM attained an accuracy of 99.26%, sensitivity of 100%, and precision value of 98.59%. Among all the F-score values obtained, the proposed

Table 2
Comparative analysis of proposed and existing techniques

Measures	Performances (%)		
	ResNet-50	DenseNet-161	UP-LSTM (Proposed)
Accuracy	91.96	91.2	99.26
Sensitivity	93.64	89.59	100
Precision	94.58	95.34	98.59
Specificity	88.28	93.56	98.46
F-score	94.11	92.38	99.29
BAC	90.96	91.57	99.23

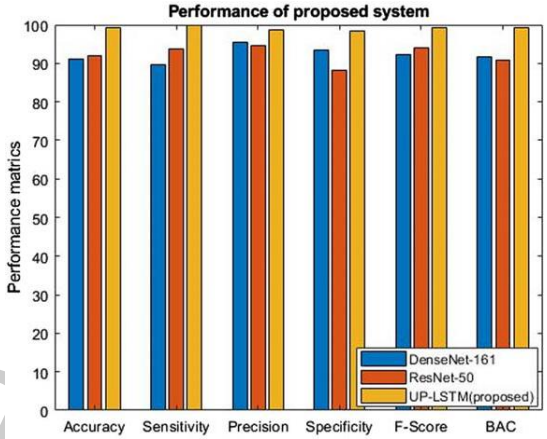

Fig. 5. Comparative analysis of proposed and existing techniques performance.

model achieves 99.29 which is better than the existing works. The average percentage obtained for the proposed model in terms of sensitivity, precision, and accuracy are 100%, 98.2% and 99.2% respectively which are better than the other compared works The performance comparisons of existing and proposed classifier with the use of test data are represented in Table 2. Therefore, the proposed classifier networks performed better than existing techniques in the breast cancer detection.

The various traditional techniques for breast cancer prediction using deep learning approaches are examined in the work for the detection of breast cancer using the similar histopathology image dataset. The layered CNN architecture is used in the work to perform an efficient detection process. The work proposed in [18] attained F-measure value of about 71.8% for CNN 3-layer architecture with the BAC of about 84.23%. The input parameters used in the work are convolutional layers which accepts labeled image data as input, 16 windows of 3x3 size filter and activation function to learn the image features. Deep learning method used in [19] that were derived from

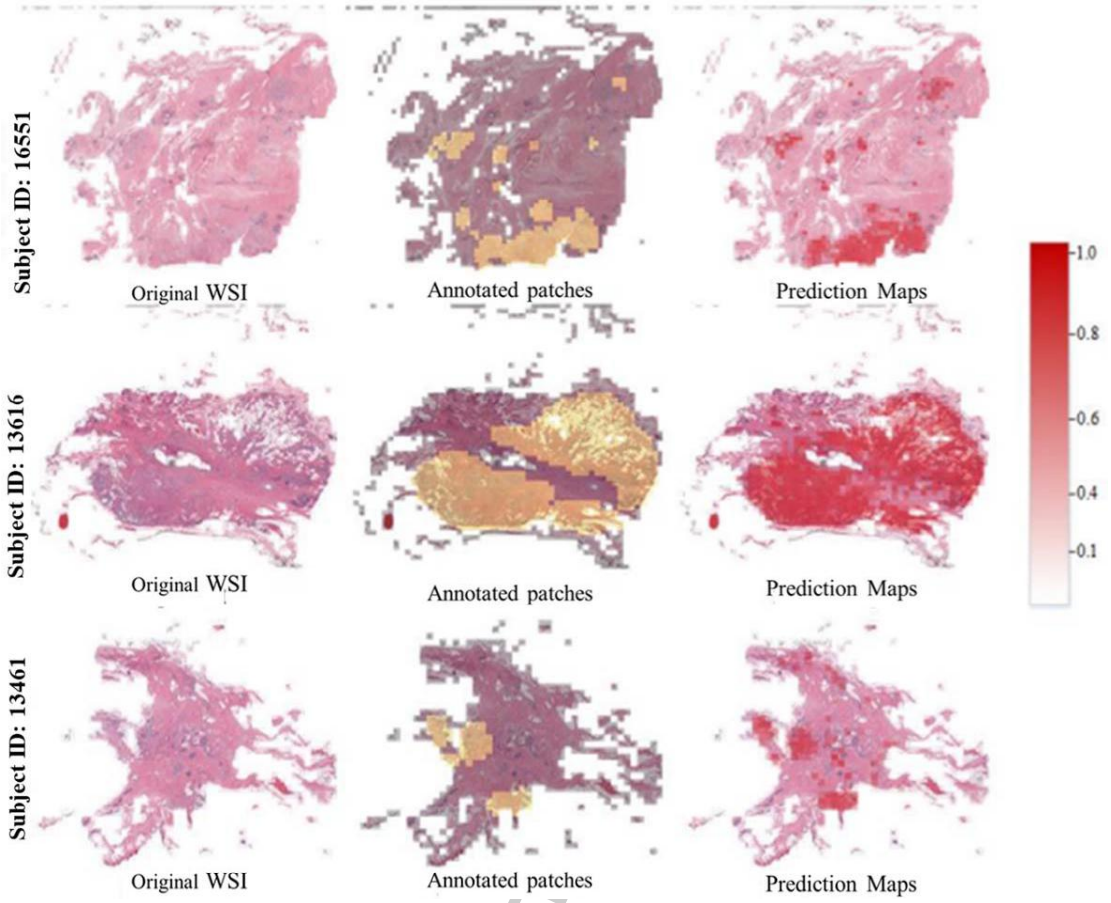

Fig. 6. Prediction maps for WSI samples in test set attained by UP-LSTM classifier model.

the architecture of inception. In the offered approach, they positioned a multilevel batch normalization layer between every layer of convolution on behalf of feature extraction. This study consist the input parameters of 5 convolutional layers, 5 max pool layers and 3 fully connected layers and aims to resize the image dataset in to 2x2 breast MRI images. The reported performance values of 89.7% and 89.00%, for F-score and BAC correspondingly. [21] uses AlexNet which is a 8-layer architecture by 32×32 input size for detection of IDC. They employed the ReLu activation function for the process detection. They attained F-score value of 76.48% and BAC value of 84.68%. The similar work in divided patch-dependent IDC data randomly as 70% training and testing 30%. They employed several under-sampling and over-sampling approaches for preventing harmful possessions of imbalanced class data on the performance of network. They attained F-score 84.78% and performance BAC 85.48% by means of their CNN 7 layer with unreal over-sampling (SMOTE) method. Table 3 offers the attained comparison table for the detection of automated IDC with the use of similar database. In addition, a deep transfer learning dependent method has been projected for IDC detection. In the work, they used D-CNN and achieved 94.11% F-score, and 90.96% BAC. Another similar work uses Multinet and achieved 98% F-score and 100% BAC. In this study UP-LSTM classifier model is employed which offers accuracy of 99.26%, sensitivity of 100%, and F-measure value of 99%. Using the proposed classifier network, a high-performance rate is attained at which the generalized ability of network is accurately measured.

Figure 7 shows the comparison of encryption time with existing work such as RSA, DES and AES algorithm. The encryption time values are compared with the RSA, DES, AES and the proposed algorithm that are in the sizes of 25KB, 50KB, 1MB, 2MB, and 3MB. This statistical result shows that the proposed

Table 3
Comparative analysis of proposed technique with previous state-of-the-art studies

Study	Input size	Method	Performance values (%)	
			F-Score	BAC
Man R et al. (2020)	50×50	3-layer CNN	71.8	84.23
Wang et al. (2020)	32×32	AlexNet	76.48	84.68
Hamsagayathri et al. (2017)	50×50	SMOTE+CNN	84.78	85.48
Valkonen et al. (2020)	50×50	Multi-level batch normalization	89.7	89
Celik, Y et al. (2020)	50×50	Transfer Learning-(DenseNet-161)	92.38	91.57
Begum A et al. (2022)	50×50	D-CNN (Deep CNN)	98	100
Khan et al. (2022)	50×50	MultiNet	99	99
Proposed	50×50	UP-LSTM (Proposed)	99.29	99.23

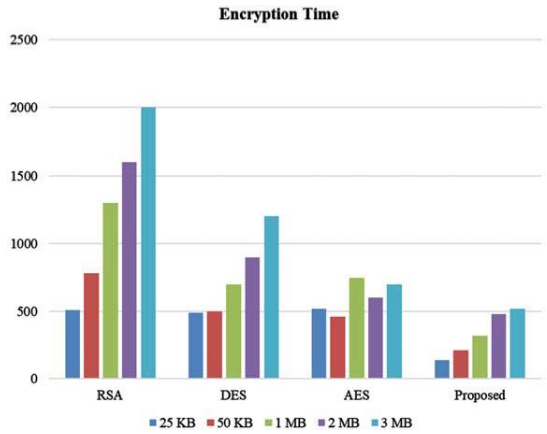

Fig. 7. Comparison of Encryption time with existing.

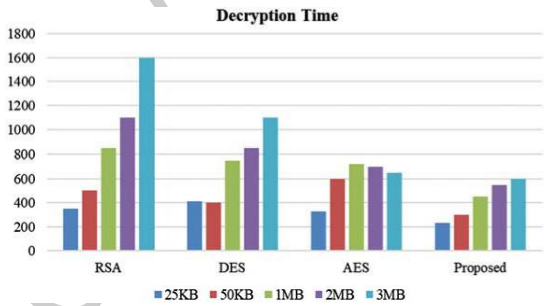

Fig. 8. Comparison of Decryption time with existing.

method takes minimum amount of time to encrypt the data in cloud. The proposed method takes 145 s for 25kb data size and 520 s for 3MB data size. It proves that the large file takes maximum amount of time to encrypt the file.

Figure 8 shows the comparison of decryption time with the existing work such as RSA, DES and AES algorithm. The decryption time values are compared with the RSA, DES, AES and the proposed an algorithm that are in the sizes of 25KB, 50KB, 1MB, 2MB, and 3MB. This statistical result shows that the proposed method takes a minimum amount of time to decrypt the data in cloud. The proposed method takes 231 s for 25kb data size and 600 s for 3MB data size. It proves that the large file takes a maximum amount of time to decrypt the file.

5. Conclusion

Automated Breast cancer screening is a more complex task for improving patient care. In this paper, the breast cancer prediction empowered with UP-LSTM classifier is employed using histopathology images. The breast image dataset is used for image preprocessing, segmentation, feature extraction, feature selection and classification. Initially, the image was preprocessed and Gaussian filtering is applied to enhance the quality of image. The experiment carried out by using the simulation of MATLAB. From the analysis, the classifier model UP-LSTM offers accuracy of 99.26%, sensitivity of 100%, and precision value of 98.59%. Moreover, Bio-inspired Iterative Honey Bee (BI-IHB) algorithm is used for ciphering the predicted data stored in cloud, which results in high security. At the same time, encryption time and decryption time have been estimated for the proposed algorithm. Also, the reliability of the detection system is verified by means of employing FMEA analysis. Using the proposed classifier network, a high-performance rate is attained at which the generalized ability of network is accurately measured. We plan to extend our in the near future by using fuzzed deep learning concepts to provide better performance in terms of computational cost, and time.

Conflict of interest

Authors declare no conflict of interests

References

[1] A. Al-Yousef and S. Samarasinghe, A Novel Computational Approach for Biomarker Detection for Gene Expression-Based Computer-Aided Diagnostic Systems for Breast Cancer, in: *Artificial Neural Networks*, Humana, New York, NY, 2021, pp. 195–208.

[2] N. Bayramoglu and J. Heikkilä, Transfer learning for cell nuclei classification in histopathology images, In: *European Conference on Computer Vision,* ECCV 2016. Springer, Cham 2016.

[3] D. Anand Golatkar and A. Sethi, Classification of breast cancer histology using deep learning, In: *International Conference Image Analysis and Recognition,* ICIAR 2018. Springer, Cham 2018.

[4] S. Vesal, N. Ravikumar, A. Davari, S. Ellmann and A. Maier, Classification of breast cancer histology images using transfer learning, In: *International Conference Image Analysis and Recognition,* ICIAR 2018. Springer, Cham 2018.

[5] G. Carneiro, Y. Zheng, F. Xing and L. Yang, Review of deep learning methods in mammography, cardiovascular, and microscopy image analysis, In: Lu L., Zheng Y., Carneiro G., Yang L and editors, *Deep Learning and Convolutional Neural Networks for Medical Image Computing [Internet]*. Switzerland: Springer; 2017.

[6] J.A. Sidey-Gibbons and C.J. Sidey-Gibbons, Machine learning in medicine: a practical introduction, *BMC Med Res Methodol* **21** (2021), 128.

[7] R. Dhumale, N. Thombare and P. Bangare, Machine Learning: A Way of Dealing with Artificial Intelligence, In: *1st International Conference on Innovations in Information and Communication Technology,* ICIICT 2019. IEEE, India 2019.

[8] WHO: New global breast cancer initiative highlights renewed commitment to improve survival [Online]. Available from: https://www.who.int/news/item/08-03-2021-new-global-breast-cancer-initiative-highlights-renewed-commitment-to-improve-survival [Accessed 11 June 2020].

[9] Basic Medical Key: Neoplasms and Cancer [Online]. Available from: https://basicmedicalkey.com/neoplasms-and-cancer [Accessed 11 June 2020].

[10] American Cancer Society: Breast Cancer Risk and Prevention [Online]. Available from: https://www.cancer.org/cancer/breast-cancer/risk-and-prevention.html [Accessed 11 June 2020].

[11] Cancer Statistics Center: [Onllne]. Available from: https://cancerstatisticscenter.cancer.org [Accessed 11 June 2020].

[12] American Cancer Society: Cancer Facts & Figures 2020 [Online]. Available from: https://www.cancer.org/content/dam/cancer-org/research/cancer-facts-and-statistics/annual-cancer-facts-and-figures/2020/cancer-facts-and-figures-2020.pdf [Accessed 11 June 2020].

[13] J. Mathana Sundarambal, S. Subramanian, H. Sandesh and G. Omprakash, A Detailed Investigation on Reduction of False Positive Rate in Breast Cancer Detection, In: *6th International Conference on Advanced Computing and Communication Systems, ICACCS 2020. IEEE*, India 2020.

[14] UCI: Breast Cancer Wisconsin (Diagnostic) Data Set; 1995. Available from: https://archive.ics.uci.edu/ml/datasets/Breast+Cancer+Wisconsin+(Diagnostic), [Accessed on 11/06/2020].

[15] H. Chang Ko, Interactive visualization of healthcare data using tableau, *Healthcare Inf Res* **23** (2017), 349–354.

[16] A. Tiwari Bhardwaj, M.V. Varma and M R. Krishna, An analysis of integration of hill climbing in crossover and mutation operation for EEG signal classification, In: *Proceedings of the 2015 Annual Conference on Genetic and Evolutionary Computation,* GECCO 2015 ACM, India 2015.

[17] J. Ivančáková, F. Babič and P. Butka, Comparison of different machine learning methods on Wisconsin dataset, In: *IEEE 16th World Symposium on Applied Machine Intelligence and Informatics,* SAMI 2018. IEEE, Slovakia, 2018.

[18] R. Man, P. Yang and B. Xu, Classification of Breast Cancer Histopathological Images Using Discriminative Patches Screened by Generative Adversarial Networks, *IEEE Access* **8** (2020), 155362–155377.

[19] C. Wang, S. Dong, X. Zhao, G. Papanastasiou, H. Zhang and G. Yang, SaliencyGAN: Deep learning semisupervised salient object detection in the fog of IoT, *IEEE Trans Ind Inf* **16**(4) (2020), 2667–2676.

[20] P. Hamsagayathri and P. Sampath, Performance analysis of breast cancer classification using decision tree classifiers, *Int J Curr Pharm Res* **9** (2017), 19–25.

[21] M. Valkonen, J. Isola, O. Ylinen, V. Muhonen, A. Saxlin, T. Tolonen, M. Nykter and P. Ruusuvuori, Cytokeratin-supervised deep learning for automatic recognition of epithelial cells in breast cancers stained for ER, PR, and Ki-67, *IEEE Trans Med Imaging* **39** (2) (2020), 534–542.

[22] Z. Han Wei, X. He and Y. Yin, Deep learning model based breast cancer histopathological image classification, In: *Proceedings of the IEEE 2nd international conference on cloud computing and big data analysis,* ICCCBDA 2017. IEEE, Chengdu 2017.

[23] A. Basavanhally Cruz-Roa, F. González, H. Gilmore, M. Feldman, S. Ganesan, et al., Automatic detection of invasive ductal carcinoma in whole slide images with convolutional neural networks, In *Medical Imaging 2014: Digital Pathology*, California 2014.

[24] K. Paeng, S. Hwang, S. Park and M. Kim, A unified framework for tumor proliferation score prediction in breast histopathology, In: *Deep Learning in Medical Image Analysis and Multimodal Learning for Clinical Decision Support,* DLMIA 2017. Springer, Cham, 2017.

[25] L. Zhang, I. Thapa, C. Haas and D. Bastola, Multiplatform biomarker identification using a data-driven approach enables single-sample classification, *BMC Bioinformatics* 20 (2019), 601.

[26] Y. Xie, F. Xing, X. Kong, H. Su and L. Yang, Beyond classification: structured regression for robust cell detection using convolutional neural network, In: *Proceedings of the International Conference on Medical Image Computing and Computer-Assisted Intervention,* MICCAI 2015. Springer, Cham 2015.

[27] F.A. Spanhol, L.S. Oliveira, C. Petitjean and L. Heutte, A dataset for breast cancer histopathological image classification, *IEEE Transactions on Biomedical Engineering* **63** (2016), 1455–1462.

[28] Y. Celik, M. Talo, O. Yildirim, M. Karabatak and U.R. Acharya, Automated invasive ductal carcinoma detection based using deep transfer learning with whole-slide images, *Pattern Recognition Letters* **133** (2020), 232–239.

[29] A. Madabhushi Janowczyk, Deep learning for digital pathology image analysis: A comprehensive tutorial with selected use cases, *J Pathol Inform* **7** (2016), 29.

[30] M.S. Reza and J. Ma, Imbalanced histopathological breast cancer image classification with convolutional neural network, In *Proceeding of the 14th IEEE International*

Conference on Signal Processing, ICSP 2018 IEEE, China 2018.

[31] A. Begum et al. A Combined Deep CNN: LSTM with a Random Forest Approach for Breast Cancer Diagnosis, *Complexity, Hindawi,* Volume **2022** | Article ID 9299621

[32] Khan et al., MultiNet: A deep neural network approach for detecting breast cancer through multi-scale feature fusion, *Journal of King Saud University – Computer and Information Sciences* **34**(8) (2022), 6217–6228

[33] Jiusi Zhang, Yuchen Jiang, Hao Luo and Shen Yin, Prediction of material removal rate in chemical mechanical polishing via residual convolutional neural network, *Control Engineering Practice* **107** (2021), 104673.

[34] Jiusi Zhang, Yuchen Jiang, Shimeng Wu, Xiang Li, Hao Luo and Shen Yin, Prediction of remaining useful life based on bidirectional gated recurrent unit with temporal self-attention mechanism, *Reliability Engineering & System Safety* **221** (2022), 108297.